# Solid Solution Creep Behavior of Sn-*x*Bi Alloys

D. MITLIN, C.H. RAEDER, and R.W. MESSLER, Jr.

This study details the steady-state creep properties of Sn-1 wt pct Bi, Sn-2 wt pct Bi, and Sn-5 wt pct Bi as a function of stress and temperature. All data, including previous work on pure Sn, are described by the following empirical equation:

$$\dot{\varepsilon}_{ss} = \frac{\mathrm{CE}}{\mathrm{R}T} \sinh\left(\frac{\alpha\sigma}{E}\right) \exp\left(\frac{-Q}{\mathrm{R}T}\right) \quad [1]$$

Equation [1] describes steady-state creep where at low strain rates there is linear stress dependence and at high strain rates there is an exponential stress dependence. The transition in creep behavior occurs at a critical, breakaway stress, $\sigma_c = E/\alpha$. This stress is compared to the breakaway stresses proposed by Friedel and by Cottrell and Jaswon. There is good agreement at low solute concentrations to the breakaway stress proposed by Friedel, but $\sigma_c$ is significantly lower than the breakaway stress predicted by Cottrell and Jaswon. Several observations suggest that for Sn-*x*Bi alloys, dislocation climb is the rate-limiting mechanism in the nonlinear region. First, the stress sensitivity of the steady-state strain rate data is similar to that of pure Sn, where dislocation climb is known to be the rate-limiting mechanism. Second, primary creep is observed throughout the tested stress range. Third, incremental additions of Bi decrease the steady-state creep rates, even though Bi has a higher diffusivity in Sn than Sn by self-diffusion.

## I. INTRODUCTION

TIN (Sn) has played a historic role in furthering the understanding of creep phenomena. In 1936, single-crystal Sn was used by Chalmers[1] to determine the exact nature and characteristics of the yield point of a material. Chalmers sought to determine whether there actually exists an exact yield point for materials, or whether its measured value is merely a function of the accuracy of the measurement technique. What he found was that creep occurred at all stresses. Additionally, two types of creep were observed: "microcreep" at strain rates under $1 \times 10^{-8}$ s$^{-1}$ and "macrocreep" at higher creep rates. The microcreep rate increased linearly with stress, while the macrocreep rate was found to increase with stress raised to an exponent greater than one. In 1948, Cottrell,[2] in a historic report to the London Physical Society, developed the theory that creep is a result of slow dislocation movement, citing Chalmers' microcreep data for single crystals of Sn as supporting evidence. In 1966, Harris *et al.*[3] examined the influence of Pb additions on the microcreep rates of Sn single crystals and confirmed the Cottrell–Jaswon[4] theory of microcreep in the presence of solute atmospheres. As recently as 1984, work on Sn, by Wu and Sherby,[5] provided a unified theory of Harper–Dorn and power-law creep behaviors. In addition, Sn has been used extensively to further theories of superplastic deformation. Cold-worked and recrystallized Sn-Bi alloys were used by Alden and coworkers[6,7] in pioneering work, which demonstrated the role of grain boundary sliding in superplastic creep behavior. Breen and Weertman,[8] Breen,[9] Ruano *et al.*,[10] and Frenkel *et al.*[11,12] have all addressed the creep of Sn. In some work,[5,10,13] power-law creep behavior is reported for Sn, whereas other work[8] reports an exponential stress dependence.

Recently, because of environmental concerns that could lead to the ban of Pb-containing alloys in soldering applications, much research has been done to further address the mechanical properties of Sn and Sn-based alloys. The Pb-free, Sn-based alloys are the most likely candidates for replacing Sn-Pb alloys in soldering applications. One of the chief concerns in applying a new solder alloy is its resistance to cyclic creep deformation, which results from thermal mismatch between electronics packages and substrates and/or power on/off cycles, which result in temperature cycling or temperature gradients within the electronics assembly. The lifetime of the solder joint is dependent on the amount of creep strain in the solder joint per temperature cycle. As such, it is desirable to increase the creep strength of solder alloys, most of which are Sn based.

This study sought to determine the effects of Bi solute concentration on the creep properties of cast and air-cooled Sn-*x*Bi, and to provide constitutive equations to describe the creep behavior over a wide range of stresses and temperatures. The creep data of Sn-1 wt pct Bi with a cast microstructure are contrasted to the creep data of the same alloy but with a recrystallized microstructure.

D. MITLIN, formerly Undergraduate Student, Department of Materials and Science and Engineering, Rensselaer Polytechnic Institute, Troy, NY 12180-3590, is Graduate Student, Center for Advanced Materials, Lawrence Berkeley National Laboratory, and the Department of Materials Science and Mineral Engineering, University of California, Berkeley, CA 94720. C.H. RAEDER, formerly Graduate Student, Department of Materials Science and Engineering, Rensselaer Polytechnic Institute, is Senior Process Engineer, Advanced Micro Devices, Austin, TX 78741. R.W. MESSLER, Jr., Associate Professor of Materials Science and Engineering and Director of Materials Joining, is with Rensselaer Polytechnic Institute.

Manuscript submitted December 14, 1994.

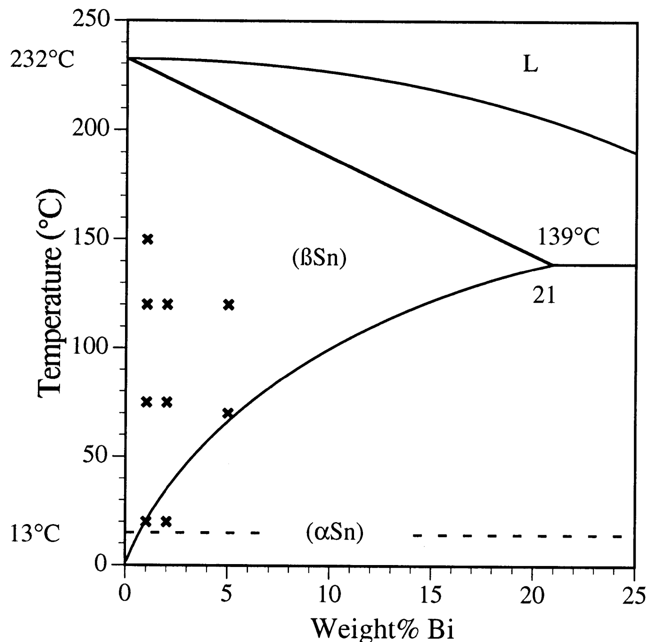


Fig. 1—Partial Sn-Bi phase diagram and test conditions (indicated by $x$).

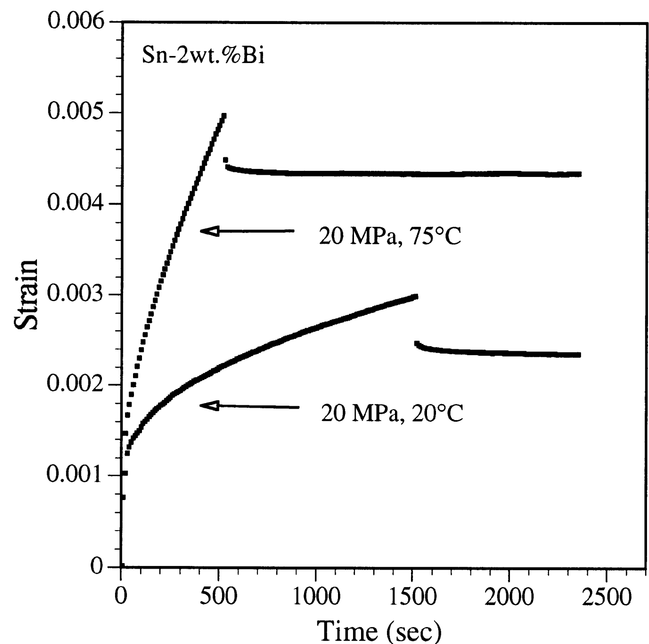


Fig. 2—Representative creep curves, taken from Sn-2 wt pct Bi creep data.

Also, this study seeks to provide an explanation of the rate controlling creep mechanisms in the cast and air-cooled Sn-$x$Bi alloys.

## II. EXPERIMENTAL PROCEDURE

Pure (99.99 pct) Sn obtained from the Indium Corporation of America (Utica, NY) and pure (99.999 pct) Bi obtained from Johnson Matthey Company (Spokane, WA) were used for all alloying. Alloys with weight additions of 1 pct Bi, 2 pct Bi, and 5 pct Bi were melted in an aluminium canister on a hot plate at a temperature of 400 °C, poured into PYREX* test tubes, and then air cooled. Examination of the aluminium canister showed that no wetting occurred, so it is reasonably assumed that there was no contamination of the Sn alloys by Al. Once cooled, the test tubes were broken and the resulting cylindrical ingots were machined into traditional dog-bone creep specimens with a 1.5-in. gage length, 0.25-in.-diameter gage section, and 0.5-in.-diameter grip section.

*PYREX is a trademark of Corning Glass Works, Corning, NY.

An Instron 4204 tensile tester with slotted grips was used for all testing. Strain in each sample was continuously monitored with an extensometer. The temperature of each test was controlled through the use of a box furnace surrounding the grip and sample assembly. Tests were performed at temperatures ranging from 20 °C to 150 °C with test temperatures varying no more than $\pm 2$ °C.

The creep tests were performed in the temperature region where there is complete solid solution of Bi in Sn (with the exception of Sn-2 wt pct Bi at 20 °C). Figure 1 shows a partial Sn-Bi phase diagram, $x$ indicating the test temperature and composition. Creep tests were conducted at constant applied load at low strain rates and at a constant displacement rate at high strain rates ($>10^{-5}$ s$^{-1}$). Primary and steady-state creep data were recorded. Following a sufficient period of steady-state creep, the stress was removed and the sample was allowed to relax for a time at least equal to the duration of the creep test. The steady-state strain rates were found by taking the slope of the linear portion of the strain *vs* time curve well after the end of transient strain and always before the onset of tertiary strain. Subsequent tests at constant temperature were run on the same sample with increasing load, so as to avoid the effects of a stable high stress microstructure on low stress tests, as reported by Langdon *et al.*[14] For constant displacement rate tests, the strain rate reported corresponds to the strain rate at which the maximum stress was achieved.

## III. RESULTS

Figure 2 shows representative creep and recovery curves taken at 20 °C and 120 °C for Sn-2 wt pct Bi. Primary (transient) creep was observed at all temperatures and stresses tested. Table I gives the composition, temperature, stress, and steady-state strain rates for all test conditions.

Figures 3(a) through (d) show the steady-state strain rate as a function of stress at various temperatures for pure Sn,[8] Sn-1 wt pct Bi, Sn-2 wt pct Bi, and Sn-5 wt pct Bi. The data do not display observable regions of constant stress dependence, making the creep rates difficult to fit with a classic power-law equation. Instead, the steady-state creep data were fit with an empirical hyperbolic sine creep relation proposed by Garofalo.[15] A similar form of the hyperbolic sine equation (with different stress exponents and pre-exponential constants) was used to describe creep data with a varying stress exponent[15] and when creep occurred by dislocation climb.[16] Also, this equation was chosen because it defines a critical transition stress ($\sigma_c < E/\alpha$) between linear and exponential regions of stress dependence. Such a transition stress will be demonstrated to occur for Sn-$x$Bi creep data.

**Table I. Steady-State Creep Data**

Column 1 = Stress (MPa)
Column 2 = Strain Rate ($s^{-1}$)

| Sn[8] (21.1 °C) | | Sn-1 Wt Pct Bi (20 °C) | | Sn-2 Wt Pct Bi (20 °C) | | Sn-5 Wt Pct Bi (70 °C) | |
|---|---|---|---|---|---|---|---|
| 5.00 | $2.76 \times 10^{-7}$ | 7.00 | $3.33 \times 10^{-9}$ | 14.0 | $9.82 \times 10^{-8}$ | 6.00 | $4.45 \times 10^{-9}$ |
| 5.70 | $4.17 \times 10^{-7}$ | 9.00 | $9.13 \times 10^{-9}$ | 20.0 | $6.95 \times 10^{-7}$ | 8.00 | $1.39 \times 10^{-8}$ |
| 5.70 | $3.33 \times 10^{-7}$ | 12.0 | $5.25 \times 10^{-8}$ | 25.0 | $4.40 \times 10^{-6}$ | 11.0 | $3.52 \times 10^{-8}$ |
| 5.70 | $3.50 \times 10^{-7}$ | 15.0 | $4.12 \times 10^{-7}$ | 30.0 | $3.75 \times 10^{-5}$ | 14.0 | $6.23 \times 10^{-8}$ |
| 7.30 | $1.10 \times 10^{-6}$ | 18.0 | $3.57 \times 10^{-6}$ | | | 18.0 | $1.73 \times 10^{-7}$ |
| 7.30 | $1.10 \times 10^{-6}$ | 22.0 | $3.49 \times 10^{-5}$ | (75 °C) | | 22.0 | $5.70 \times 10^{-7}$ |
| 9.10 | $3.02 \times 10^{-6}$ | | | 5.00 | $1.16 \times 10^{-8}$ | 28.0 | $7.08 \times 10^{-6}$ |
| 9.10 | $2.78 \times 10^{-6}$ | (75 °C) | | 7.00 | $3.07 \times 10^{-8}$ | 35.0 | $7.60 \times 10^{-5}$ |
| 9.10 | $3.13 \times 10^{-6}$ | 5.00 | $4.33 \times 10^{-9}$ | 9.00 | $7.48 \times 10^{-8}$ | 45.0 | $2.24 \times 10^{-3}$ |
| 9.10 | $3.58 \times 10^{-6}$ | 7.00 | $3.62 \times 10^{-8}$ | 12.0 | $2.37 \times 10^{-7}$ | | |
| 11.4 | $9.00 \times 10^{-6}$ | 9.00 | $1.59 \times 10^{-7}$ | 16.0 | $1.34 \times 10^{-6}$ | (120 °C) | |
| 11.4 | $1.08 \times 10^{-5}$ | 12.0 | $2.37 \times 10^{-6}$ | 20.0 | $5.42 \times 10^{-6}$ | 4.00 | $1.11 \times 10^{-8}$ |
| | | 15.0 | $2.92 \times 10^{-5}$ | 25.0 | $6.22 \times 10^{-5}$ | 5.00 | $1.65 \times 10^{-8}$ |
| (93 °C) | | 18.0 | $1.80 \times 10^{-4}$ | 30.0 | $3.32 \times 10^{-4}$ | 7.00 | $3.18 \times 10^{-8}$ |
| 4.30 | $3.17 \times 10^{-6}$ | | | | | 9.00 | $7.13 \times 10^{-8}$ |
| 5.00 | $6.17 \times 10^{-6}$ | (120 °C) | | (120 °C) | | 12.0 | $1.95 \times 10^{-7}$ |
| 5.00 | $9.83 \times 10^{-6}$ | 3.00 | $1.24 \times 10^{-8}$ | 4.00 | $4.33 \times 10^{-8}$ | 15.0 | $5.55 \times 10^{-7}$ |
| 5.70 | $6.33 \times 10^{-6}$ | 5.00 | $1.33 \times 10^{-7}$ | 5.00 | $4.92 \times 10^{-8}$ | 18.0 | $1.49 \times 10^{-6}$ |
| 5.70 | $1.25 \times 10^{-5}$ | 7.00 | $7.60 \times 10^{-7}$ | 7.00 | $1.19 \times 10^{-7}$ | 22.0 | $6.42 \times 10^{-6}$ |
| 7.30 | $4.33 \times 10^{-5}$ | 9.00 | $4.55 \times 10^{-6}$ | 9.00 | $4.22 \times 10^{-7}$ | 26.0 | $3.79 \times 10^{-5}$ |
| | | 12.0 | $6.00 \times 10^{-5}$ | 12.0 | $1.82 \times 10^{-6}$ | 30.0 | $3.97 \times 10^{-4}$ |
| | | | | 15.0 | $6.47 \times 10^{-6}$ | | |
| | | (150 °C) | | 18.0 | $2.02 \times 10^{-5}$ | | |
| | | 3.00 | $1.67 \times 10^{-7}$ | 21.0 | $7.75 \times 10^{-5}$ | | |
| | | 4.00 | $3.83 \times 10^{-7}$ | 25.0 | $3.80 \times 10^{-4}$ | | |
| | | 5.00 | $8.45 \times 10^{-7}$ | | | | |
| | | 7.00 | $5.06 \times 10^{-6}$ | | | | |
| | | 9.00 | $3.07 \times 10^{-5}$ | | | | |
| | | 12.0 | $2.66 \times 10^{-4}$ | | | | |
| | | 15.0 | $1.53 \times 10^{-3}$ | | | | |

$$\dot{\varepsilon}_{ss} = \frac{CE}{RT} \sinh\left(\frac{\alpha\sigma}{E}\right) \exp\left(\frac{-Q}{RT}\right) \qquad [1]$$

where $\dot{\varepsilon}_{ss}$ is the steady-state strain rate ($s^{-1}$), $Q$ is the creep activation energy (kJ/mole), R is the gas constant, $T$ is temperature (K), $C$ J/(mole MPa) and $\alpha$ (dimensionless) are constants, $E$ is the temperature and composition-dependent Young's modulus (MPa), and $\sigma$ is the applied stress (MPa).

The original form of Eq. [1] was $\dot{\varepsilon}_{ss} = A\ (\sinh\ (\alpha\sigma))^n$, where $n$ varied from 1 to 5.[15] The advantage of the revised form used here is that it allows calculation of the transition stress, accounts for a varying Young's modulus, and does not require the constant $C$ to change with test temperature, as $A$ did.

Values of Young's modulus for Sn-$x$Bi as a function of temperature and composition were taken from Drapkin and Kononenko.[17] The values used in data reduction and curve fitting are shown in Table II. Young's modulus data for Sn-2 wt pct Bi and Sn-1 wt pct Bi were estimated by linear interpolation of the data for pure Sn and Sn-5 wt pct Bi.

The creep activation energy for each alloy was calculated by taking the average of the slopes of the isostress lines of ln (strain rate) *vs* $1/T$. Figure 4 shows a representative plot for Sn-2 wt pct Bi. Figure 5 shows the activation energy compensated steady-state strain rate *vs* stress normalized by the Young's modulus, for Sn-$x$Bi alloys and for pure Sn.[8] The constants $C$ and $\alpha$ were obtained from a fit of Eq. [1] to the data. Table III summarizes the constitutive relation constants for pure Sn, Sn-1 wt pct Bi, Sn-2 wt pct Bi, and Sn-5 wt pct Bi. The lines in Figures 3 (a) through (d) represent the fit using Eq. [1] with the constants listed in Table III.

To show the relative effect of Bi solute on the creep strength of Sn, a Larson–Miller[18] type plot of all data is given in Figure 6. The steady-state data were collapsed with temperature using the relation $\log \sigma = T\ (C' - C''(\log \dot{\varepsilon}_{ss}))$. The constants $C'$ and $C''$ were evaluated to achieve best collapse of the data and were found to be 20 and 8, respectively. Figure 6 demonstrates the increase in the creep strength with increasing Bi alloying content.

## IV. DISCUSSION

### A. *Effect of an As-Cast versus a Recrystallized Microstructure on the Creep Properties of Sn-1 wt pct Bi*

The only previous work known to the authors on Sn-Bi solid solution creep shows distinctly different results from those reported here. Figure 7 compares the room-temperature steady-state strain rate of cast Sn-1 wt pct Bi to that reported in the literature.[7] The distinct difference is due to different microstructures used in the studies. In the earlier work,[7] the Sn-1 wt pct Bi microstructure consisted of small, equiaxed grains having an initial diameter of approximately 2 $\mu$m produced by cold working and annealing the sample. At intermediate strain rates ($10^{-8}$ to $10^{-5}$ $s^{-1}$),

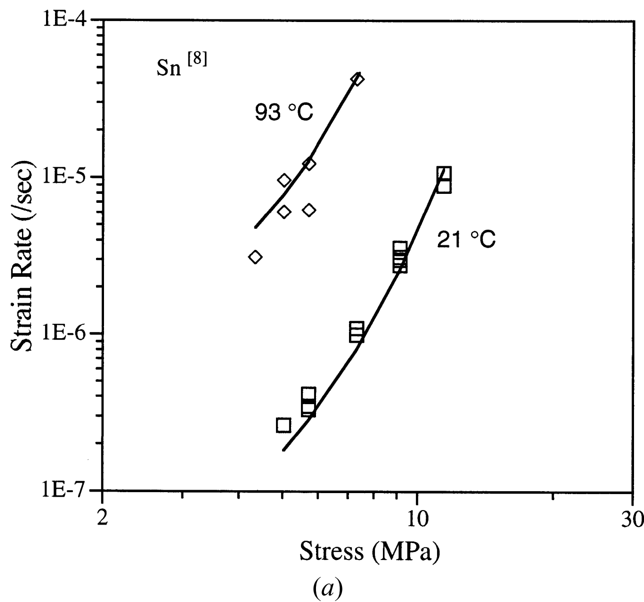

(*a*)

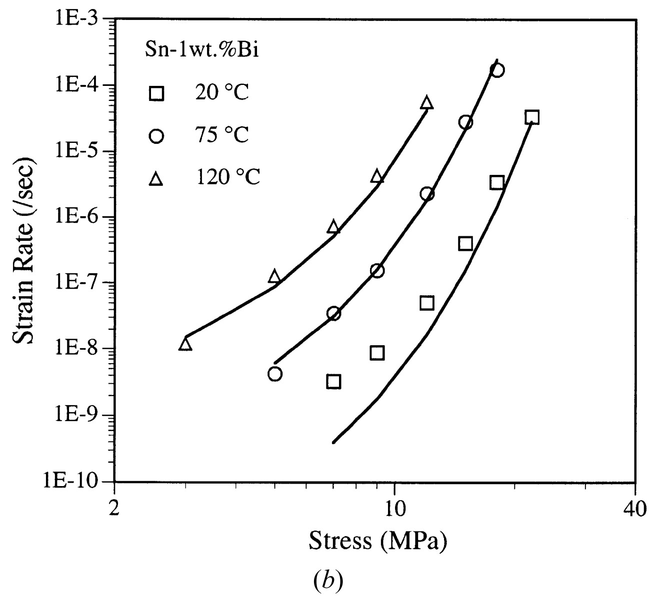

(*b*)

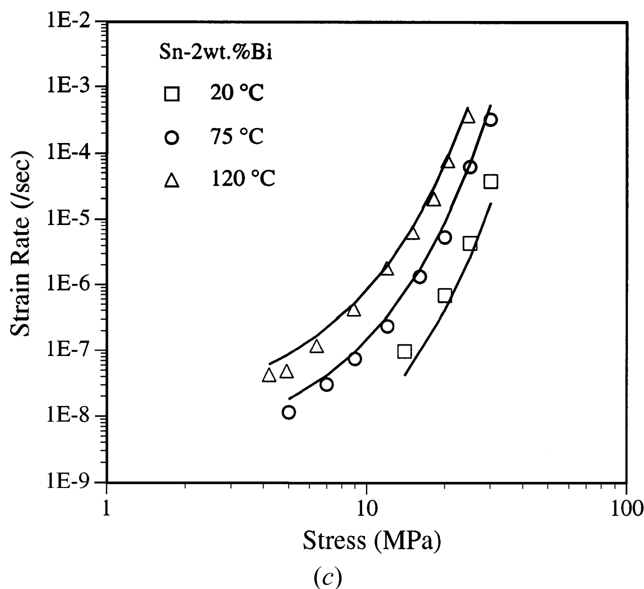

(*c*)

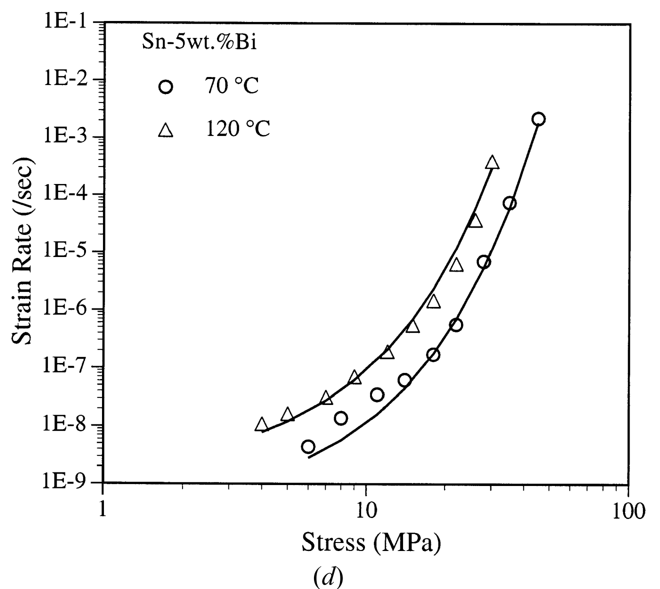

(*d*)

Fig. 3—(*a*) Steady-state strain rate and constitutive equation fit (indicated by lines) of data for pure Sn.[8] (*b*) Steady-state strain rate and constitutive equation fit (indicated by lines) of data for Sn-1 wt pct Bi. (*c*) Steady-state strain rate and constitutive equation fit (indicated by lines) of data for Sn-2 wt pct Bi. (*d*) Steady-state strain rate and constitutive equation fit (indicated by lines) of data for Sn-5 wt pct Bi.

the recrystallized and cast microstructures have significantly different dependencies of the strain rate on the flow stress. The recrystallized microstructure has a power-law stress dependence with stress exponent equal to 2.5, characteristic of superplastic deformation, while the cast microstructure has an exponential stress dependence with consistently higher slope, $n = 7$ to 10, under the same conditions of stress and temperature. Also, in this region, Sn-1 wt pct Bi with the fine-grained recrystallized microstructure displays significantly higher strain rates than that with the cast microstructure. In superplastic deformation, characteristic of recrystallized material, bulk grain strains are insignificant compared to grain boundary sliding; the deformation rate being determined by the rate at which boundary dislocations accommodate sliding, as opposed to in the cast microstructure, where movement of dislocations within the grains determines the creep rate. At high strain rates, the recrystallized and cast microstructures exhibit a similar flow stress.

These observations support and extend prior discussions[19,20,21] on the differentiation of superplastic behavior from normal creep behavior caused by the character of the grain and phase boundaries and the coarseness and morphology of the microstructure.

## B. *Creep Mechanisms in Sn-xBi Alloys*

The easiest way to assign a rate-determining mechanism during creep is to look at the stress exponent $n$ ($\dot{\varepsilon}_{ss} \propto \sigma^n$). During creep, solid solutions often behave as either a class A (alloy) or a class M (pure metal) material. Class A materials display a characteristic power-law exponent approximately equal to 3, which is associated with dislocation glide as the rate-determining mechanism. Creep strength-

**Table II. Young's Modulus (GPa) of Sn-*x*Bi Alloys[17]**

| Alloy/Temperature | 20 °C | 70 °C, 75 °C, or 93 °C | 120 °C |
|---|---|---|---|
| Sn | 54.2 | 48.3 (93.3 °C) | 45.5 |
| Sn-1 wt pct Bi | 53.6 | 49.0 (75) | 45.3 |
| Sn-2 wt pct Bi | 53.0 | 48.5 (75) | 45.1 |
| Sn-5 wt pct Bi | 52.5 | 48.5 (70) | 44.5 |

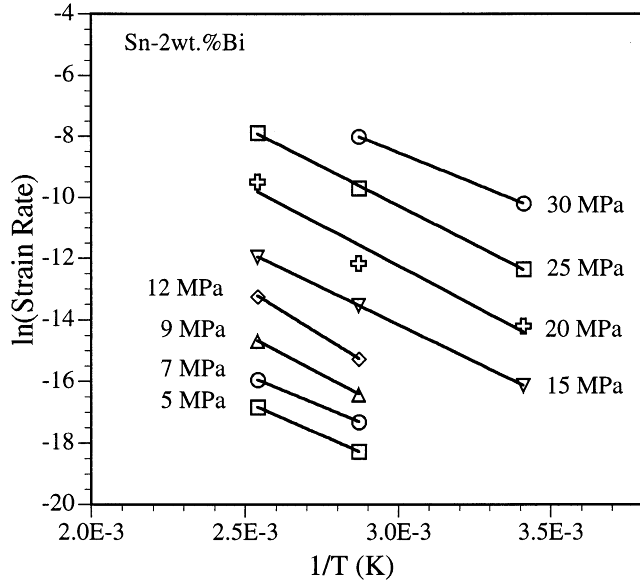


Fig. 4—Arrhenius plot of Sn-2 wt pct Bi creep data, used for determination of the creep activation energy.

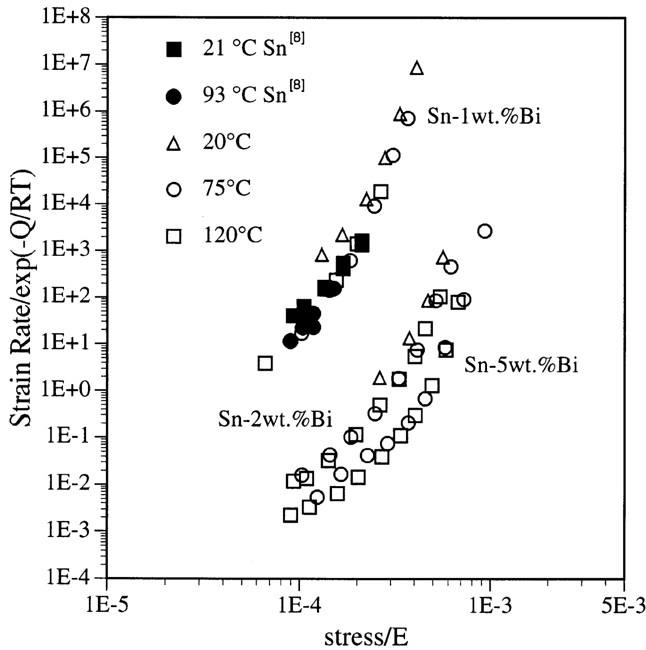


Fig. 5—The activation energy compensated steady-state strain rate *vs* stress normalized by the Young's modulus, for Sn-*x*Bi alloys and for Sn.[8]

**Table III. Constitutive Equation Constants for Sn-*x*Bi Alloys**

| Alloy | *C* (J K/mole MPa) | $\alpha$ | *Q* (kJ/mole) |
|---|---|---|---|
| Sn[8] | $1 \times 10^{-1}$ | 35,000 | 46.1[8] |
| Sn-1 wt pct Bi | $5 \times 10^{-2}$ | 40,000 | 64 |
| Sn-2 wt pct Bi | $4 \times 10^{-4}$ | 20,000 | 41 |
| Sn-5 wt pct Bi | $5 \times 10^{-5}$ | 18,000 | 40 |

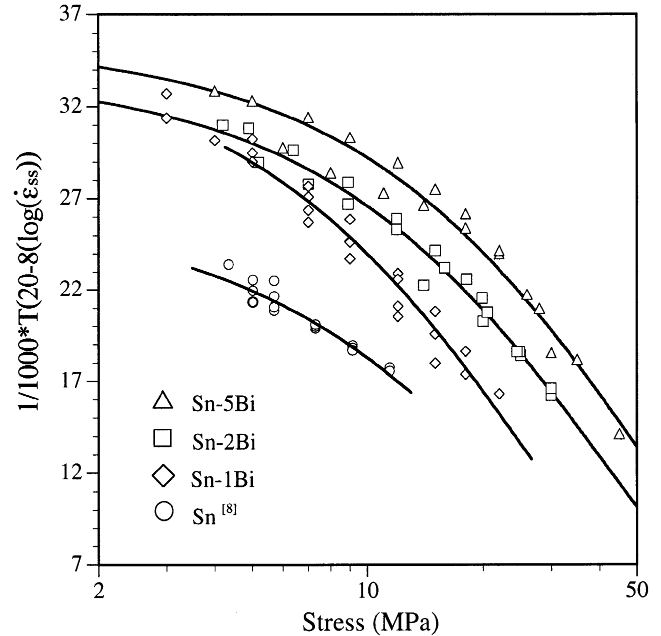


Fig. 6—Master curve of Larson–Miller[18] type parameter for steady-state creep.

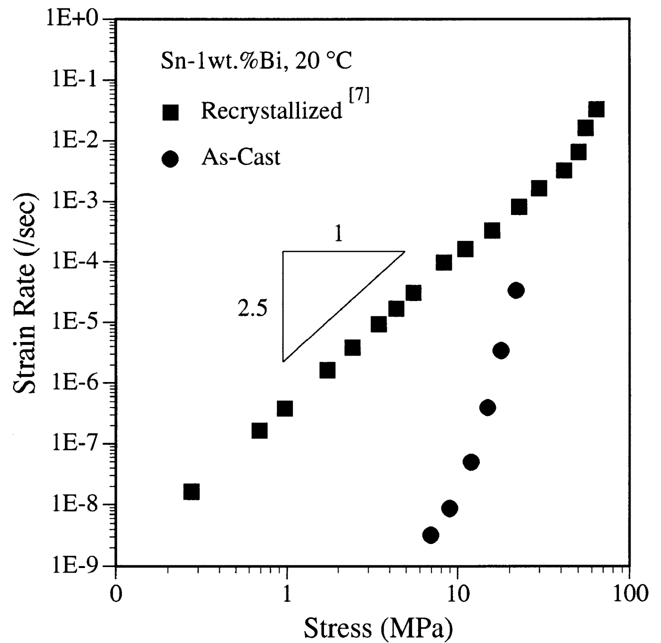


Fig. 7—A comparison of the creep properties of Sn-1 wt pct Bi having an as-cast *vs* a recrystallized[7] microstructure.

ening from solute additions comes from the ability of the solute atmospheres to segregate to dislocations and reduce their rate of glide. To have this effect, the solute must have a lower diffusivity than the self-diffusion rate of the base metal, since creep rate is determined by the fastest diffusing species. Class A materials do not display significant primary (transient) creep.

Class M materials typically display a power-law expo-

nent between 5 and 7. As for pure metals, the rate-determining mechanism in class M materials is dislocation climb. Solid solution strengthening is achieved by a reduction of the stacking fault energy, thereby decreasing the rate of dislocation climb. Creep rate is determined by the slowest diffusing species. Class M materials display significant primary creep.

As mentioned previously, no one stress exponent describes the Sn-$x$Bi creep data, making the discussion of possible rate-determining creep mechanisms difficult. However, several observations suggest that dislocation climb may be the creep rate determining mechanism throughout the majority of the stress regime tested. From Figures 3 (a) through (d) and 5, it can be seen that with the exception of the low stress regime in Sn-2 wt pct Bi and Sn-5 wt pct Bi, the stress sensitivity of the steady-state strain rate data is similar to that of pure Sn, where dislocation climb is rate determining.[13]

The second reason that dislocation climb is the most likely rate-determining creep mechanism is that Bi diffuses faster in Sn than Sn self-diffuses. The activation energies for creep of Sn can be grouped into a high-temperature creep activation energy, $T > 150$ °C and a low-temperature creep activation energy, $T < 120$ °C, with a transition region in between.[8,12,13,22,23] Table IV summarizes these findings. The high-temperature activation energies closely correspond to those reported for self-diffusion, given in Table V.

**Table IV. Activation Energy for Creep of Sn at High and Low Temperatures**

| Source | Temperature Range (° C) | Activation Energy (kJ/mole) |
|---|---|---|
| Breen and Weertman[8] | 160 to 224 | 108.8 |
| Mohamed, Murty and Morris[13] | 129 to 222 | 95.52 |
| Frenkel, Sherby and Dorn[12] | 100 to 205 | 87.86 |
| Bonar and Craig[22] | 27 to 77 | 37.66 |
| Breen and Weertman[8] | 20 to 90 | 46.02 |
| | 90 to 160 | transition |
| Rotherham, Smith and Greenough[23] | 15 to 150 | 46.03 |

If in the 20 °C to 120 °C temperature range dislocation glide is the rate-determining mechanism in Sn-$x$Bi alloys, then the diffusivity of Bi in Sn must be less than that of Sn self-diffusion; otherwise, no strengthening would be observed. Diffusion constants and activation energies of Sn self-diffusion[24,25] and tracer diffusion of Bi in Sn[26] are shown in Table V with the corresponding diffusivities at 20 °C, 75 °C, and 120 °C. The Sn self-diffusion activation energies correlate well with the activation energies for creep of Sn observed in the same high-temperature range. The calculated diffusivities of Bi in Sn are several orders of magnitude larger than the calculated values of Sn self-diffusion, indicating that additions of Bi to Sn would not decrease its creep rate if dislocation glide was the rate-limiting mechanism.

Finally, primary creep is observed throughout the entire stress and temperature regime that was tested. Figure 8 shows the primary creep strain as a function of stress, measured from the creep curves of Sn-2 wt pct Bi. The amount of primary creep increases with increasing stress.

Prior studies of Sn and Sn alloys[1–5,10,13] show that a critical stress exists above which a transition from a linear stress dependence to either power-law or exponential behavior occurs. This breakdown in linear dependence is explained as a breakaway of the dislocations from their solute atmospheres.[1–4] When the data are described as they are here, the experimental breakaway stress for Sn-$x$Bi alloys is given by the condition $\sigma = E/\alpha$. These values may be compared to those predicted by Friedel,[27] and by Cottrell and Jaswon.[4] The breakaway stress for unsaturated dislocations was derived by Friedel[27] as

$$\tau_b = (A_b W_m^2/\mathrm{k}T\mathbf{b}^3)C_o \quad [2]$$

where $\tau_b$ is the shear stress necessary to separate a dislocation from its solute atmosphere, k is the Boltzmann constant, **b** is the Burgers vector having a value of 3.18 Å,[27] $W_m$ is the interaction energy between a solute atom and an edge dislocation, and $C_0$ is the atomic concentration of the

**Table V. Self and Tracer Diffusion Activation Energies and Coefficients**

| Method | $D_o$ (cm² sec⁻¹) | $Q$ (kJ/mole) | $T$ (°C) | $D$ (cm² sec⁻¹) |
|---|---|---|---|---|
| Sn113, 99.999% 160–228 °C[24] | ($c$-axis) 7.7 | (c) 106.9 | 20 | 6.73E-19 |
| | | | 75 | 6.92E-16 |
| | | | 120 | 4.76E-14 |
| Sn113, 99.999% 160–228 °C[24] | ($a$-axis) 10.7 | (a) 105.0 | 20 | 2.04E-18 |
| | | | 75 | 1.86E-15 |
| | | | 120 | 1.18E-13 |
| Sn113, 99.999% 152–227 °C[25] | ($c$-axis) 12.8 | (c) 108.9 | 20 | 5.80E-19 |
| | | | 75 | 6.62E-16 |
| | | | 120 | 4.85E-14 |
| Sn113, 99.999% 152–227 °C[25] | ($a$-axis) 21.0 | (a) 107.9 | 20 | 1.22E-18 |
| | | | 75 | 1.34E-15 |
| | | | 120 | 9.56E-14 |
| Bi in Sn 167–220 °C[26] | (polycrystal) 72.0 | 76.12 | 20 | 1.93E-12 |
| | | | 75 | 2.70E-10 |
| | | | 120 | 5.49E-09 |

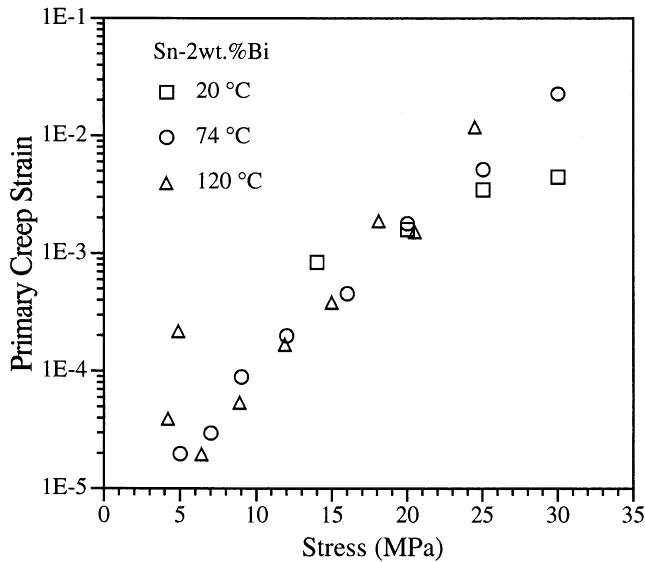


Fig. 8—Primary creep strain *vs* stress for Sn-2 wt pct Bi.

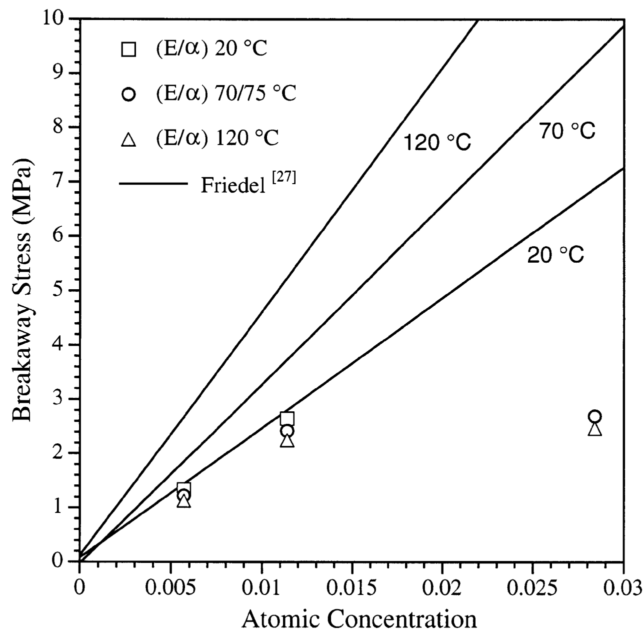


Fig. 9—Dislocation breakaway stress calculated from a constitutive equation and that predicted by Friedel.[27]

solute. The term $A_b$ is a dimensionless constant, calculated by Endo *et al.* to be 0.1.[29] Friedel defined $W_m$ as follows:[27]

$$W_m = -\frac{1}{2\pi}\left(\frac{1+\mu}{1-\mu}\right)G|\Delta V| \qquad [3]$$

where $\mu$ is the Poisson's ratio equal to 0.33,[27] $G$ is the shear modulus, and $\Delta V$ is the volume difference between a solute and a solvent atom (atomic radius of Bi is 1.63 Å, and atomic radius of Sn is 1.72 Å).

Cottrell and Jaswon[4] derived an analogous but separate expression for breakaway stress given by

$$\sigma_c = 27\left(\frac{1}{\mathbf{b}}\right)\mathrm{k}TC_oLN \qquad [4]$$

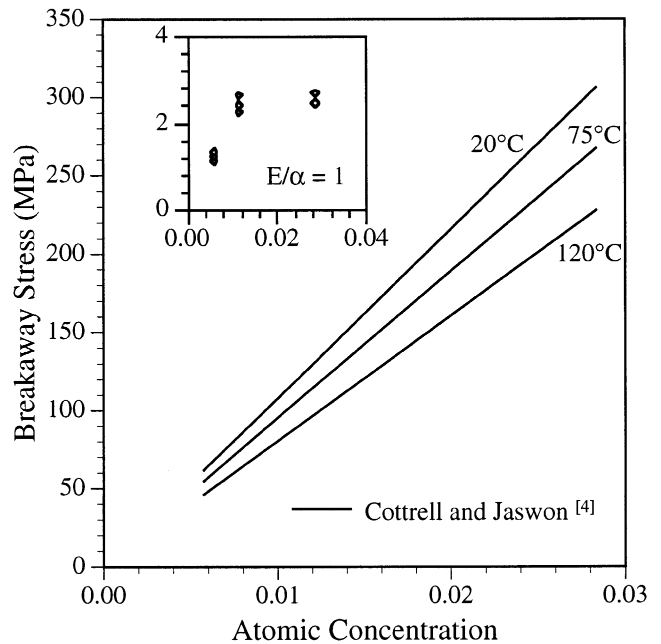


Fig. 10—Dislocation breakaway stress calculated from a constitutive equation and that predicted by Cottrell and Jaswon.[4]

where $N$ is the number of atom sites per unit volume, 1.84 $\times$ $10^{28}$ $m^{-3}$ (Sn has two atoms per unit cell, $a = b = 5.8317$ Å, and $c = 3.1815$ Å) and $L$ is the distance by which a solute atmosphere must lag in order for the dislocation to attain critical velocity. Cottrell defined $L$ by the following equation:[28]

$$L = 4\,\frac{D\rho\mathbf{b}}{\dot{\varepsilon}_{\mathrm{crit}}} \qquad [5]$$

where $D$ is the diffusivity and $\rho$ is the dislocation density. Using Chalmers data for Sn,[2] the critical strain rate is $10^{-8}$ $s^{-1}$, and $D\rho$ is equal to $10^{-8}$ $s^{-1}$. Hence, $L$ is equal to 4**b**.

Figure 9 compares the Friedel breakaway stress calculated from Eq. [2] (converted to tensile using $\sigma = 3^{1/2}\tau$) to that obtained from the constitutive creep equations of the Sn-*x*Bi alloys ($\sigma = E/\alpha$). Figure 10 compares the breakaway stress calculated from Eq. [4] to $E/\alpha$. The Friedel breakaway stress values are in reasonable agreement with the experimental values at low Bi concentrations, while the Cottrell and Jaswon[4] breakaway stress values are more than an order of magnitude too high. The Sn-5 wt pct Bi data deviate significantly from both predictions. This effect may be due to a saturation of Bi solute at the dislocation cores; no more strengthening may be achieved with increasing solute content. This agrees with previous experiments done on breakaway stress in Al-*x*Mg alloys.[29] Alternatively, this discrepancy may be due to a transition to another rate-determining creep mechanism. In Sn-5 wt pct Bi, and in Sn-2 wt pct Bi to a lesser extent, there appears to be a low stress region, where the shape of the strain rate *vs* stress curve is distinctly different from that of pure Sn (Figure 5). This suggests a region where other mechanisms may be rate determining. For example, a region of limited superplasticity ($n$ is approximately 2.5) or dislocation glide ($n$ is approximately 3) may yield a weaker stress dependence that is observed at low stresses.

## V. SUMMARY AND CONCLUSIONS

1. The creep properties of Sn were investigated as a function of Bi content. In the 1 to 5 wt pct concentration range, Bi improves the creep strength of Sn.
2. The steady-state creep data are well described by a hyperbolic sine relation, which is characterized by a linear stress dependence at low strain rates and an exponential stress dependence at high strain rates.
3. The steady-state creep data of Sn-1 wt pct Bi were compared to those previously reported by Alden.[6] The present data show a far greater stress dependence and greater creep strength at intermediate stresses. These differences are attributed to microstructural considerations. Prior data were collected on samples of fine-grained recrystallized material as opposed to the material used presently, which was in its cast state.
4. At high stresses, dislocation climb may be the rate-limiting mechanism in Sn-*x*Bi alloys. The transition stress from a linear stress dependence of the steady-state strain rate to an exponential stress dependence is believed to be the stress at which dislocations break away from their solute atmospheres. This breakaway stress is most accurately described by Friedel,[27] while the predictions by Cottrell and Jaswon[4] yield values more than an order of magnitude too high.


## ACKNOWLEDGMENTS

The authors thank Professor J.W. Morris, Jr., Professor Daeyong Lee, Dr. Don Millard, Dr. Heidi Davis, and Mr. Don Van Steele for their advice and technical support. The authors also thank the sponsors of the Electronics Manufacturing Program, CIEEM, Rensselaer Polytechnic Institute, the United States Army, AT&T, Boeing, Navy Mantech, Northern Telecom, and Thomson Electronics, without whose generous support this work would not have been possible.


## REFERENCES


1. B. Chalmers: *Proc. R. Soc.*, 1936, vol. A156, pp. 427-43.
2. A.H. Cottrell: *Conf. on Strength of Solids*, Physics Society, London, 1948, pp. 30-38.
3. A. Harris, R.L. Hines, and E.R. Peck: *Acta Metall.*, 1966, vol. 14, pp. 1115-19.
4. A.H. Cottrell and M.A. Jaswon: *Proc. R. Soc.*, 1949, vol. A199, pp. 104-14.
5. M.Y. Wu and O.D. Sherby: *Acta Metall.*, 1984, vol. 32, pp. 1561-72.
6. T.H. Alden: *Acta Metall.*, 1967, vol. 15, pp. 469-80.
7. M.A. Clark and T.H. Alden: *Acta Metall.*, 1973, vol. 21, pp. 1195-1206.
8. J.E. Breen and J. Weertman: *Trans. AIME*, 1955, vol. 203, pp. 1230-34.
9. J.E. Breen: Master's Thesis, University of Maryland, College Park, MD, 1954.
10. O.A. Ruano, J. Wadsworth, and O.D. Sherby: *Acta Metall.*, 1988, vol. 36, pp. 1117-28.
11. R.E. Frenkel, O.D. Sherby, and J.E. Dorn: *Acta Metall.*, 1955, vol. 3, pp. 470-72.
12. R.E. Frenkel, O.D. Sherby, and J.E. Dorn: Institute of Engineering Research Report, University of California, Berkeley, CA, 1954, series no. 22, issue no. 36.
13. F.A. Mohamed, K.L. Murty, and J.W. Morris, Jr.: *Metall. Trans. A*, 1973, vol. 4A, pp. 935-40.
14. T.G. Langdon, R.B. Vastava, and P. Yavari: *Proc. 5th Int. Conf. on the Strength of Metalls and Alloys*, P. Haasen, V. Gerold, and G. Kostorz, eds., Permagon, Oxford, United Kingdom, 1980, vol. 1, pp. 271-76.
15. F. Garofalo: *Trans. TMS-AIME*, 1963, vol. 227, pp. 351-55.
16. J. Weertman: *J. Appl. Phys.*, 1957, vol. 28, pp. 362-64.
17. B.M. Drapkin and V.K. Kononenko: *Izv. Akad. Nauk SSSR Metally*, 1987, No. 2, pp. 168-71.
18. F.R. Larson, and J. Miller: *Trans. ASME*, 1952, vol. 74, pp. 765-75.
19. T.H. Alden: *J. Aust. Inst. Met.*, 1969, vol. 14, pp. 207-16.
20. H.E. Cline and D. Lee: *Acta Metall.*, 1970, vol. 18, pp. 315-23.
21. T.G. Langdon: *Strength of Metals and Alloys, Proc. 6th Int. Conf.*, Melbourne, Australia, Aug. 1982, Pergamon Press, NY, 1983, pp. 1105-20.
22. L.G. Bonar and G.B. Craig: *Can. J. Phys.*, 1958, vol. 36, pp. 1445-48.
23. L. Rotherham, A.D.N. Smith, and G.B. Greenough: *J. Inst. Met.*, 1951, vol. 79, pp. 439-54.
24. C. Coston and N.H. Nachtrieb: *J. Phys. Chem.*, 1964, vol. 68, pp. 2219-29.
25. H. Huang and H.B. Huntington: *Phys. Rev. B*, 1974, vol. 9, pp. 1479-88.
26. L. Holmes and W.C. Winegard: *TMS-AIME*, 1962, vol. 224, pp. 945-49.
27. J. Freidel: *Dislocations*, Permamon Press, Oxford, United Kingdom, 1964.
28. A.H. Cottrell: *Dislocations and Plastic Flow in Crystals*, Oxford University Press, Oxford, United Kingdom, 1953, p. 139.
29. T. Endo, T. Shimada, and T.G. Langdon: *Acta Metall.*, 1984, vol. 32, pp. 1991-99.